Basic structures for photonic integrated circuits in Silicon-on-insulator

W. Bogaerts, D. Taillaert, B. Luyssaert, P. Dumon, J. Van Campenhout, P. Bienstman, D. Van Thourhout and R. Baets

Ghent University - IMEC, Department of Information Technology (INTEC)
Sint-Pietersnieuwstraat 41, 9000 Gent, BELGIUM

V. Wiaux, S. Beckx

IMEC vzw., Silicon Process Technology Division
Kapeldreef 75, 3001 Leuven, BELGIUM
wim.bogaerts@intec.UGent.be

Abstract: For the compact integration of photonic circuits, wavelength-scale structures with a high index contrast are a key requirement. We developed a fabrication process for these nanophotonic structures in Silicon-on-insulator using CMOS processing techniques based on deep UV lithography. We have fabricated both photonic wires and photonic crystal waveguides and show that, with the fabrication technique, photonic wires have much less propagation loss than photonic crystal waveguides. Measurements show losses of 0.24dB/mm for photonic wires, and 7.5dB/mm for photonic crystal waveguides. To tackle the coupling to fiber, we studied and fabricated vertical fiber couplers coupling efficiencies of over 21%. In addition, we demonstrate integrated compact spot-size converters with a mode-to-mode coupling efficiency of over 70%.

OCIS codes: (250.5300) Photonic Integrated Circuits (220.4610) Optical Fabrication

---

References and links

1. J. D. Joannopolous, R. Meade, and J. Winn, *Photonic Crystals - Molding the Flow of Light* (Princeton University Press, Princeton, N.J., 1995).
2. "SOITEC's Unibond(R) process," Microelectronics Journal **27**(4/5), R36 (1996).
3. W. Bogaerts, V. Wiaux, D. Taillaert, S. Beckx, B. Luyssaert, P. Bienstman, and R. Baets, "Fabrication of photonic crystals in silicon-on-insulator using 248-nm deep UV lithography," IEEE J. Sel. Top. Quantum Electron. **8**, 928–934 (2002).
4. W. Bogaerts, V. Wiaux, P. Dumon, D. Taillaert, J. Wouters, S. Beckx, J. Van Campenhout, B. Luyssaert, D. Van Thourhout, and R. Baets, "Large-scale production techniques for photonic nanostructures," Proc. SPIE **5225**, 101–112 (2003).
5. J. Arentoft, T. Sondergaard, M. Kristensen, A. Boltasseva, M. Thorhauge, and L. Frandsen, "Low-loss silicon-on-insulator photonic crystal waveguides," Electron. Lett. **38**, 274–275 (2002).
6. M. Vaughan. *The Fabry-Perot interferometer* (Adam Hilger, Bristol, 1989).
7. P. Dumon, W. Bogaerts, V. Wiaux, J. Wouters, S. Beckx, J. Van Campenhout, D. Taillaert, B. Luyssaert, P. Bienstman, D. Van Thourhout, and R. Baets, "Low-loss SOI Photonic Wires and Ring Resonators Fabricated with Deep UV Lithography," accepted for publication in Photonics Technology Letters (2004).
8. T. Shoji, T. Tsuchizawa, T. Watanabe, K. Yamada, and H. Morita, "Low loss mode size converter from $0.3\mu m$ square Si waveguides to singlemode fibres," Electron. Lett. **38**, 1669–1700 (2002).
9. D. Taillaert, W. Bogaerts, P. Bienstman, T. Krauss, P. Van Daele, I. Moerman, S. Verstuyft, K. De Mesel, and R. Baets, "An out-of-plane grating coupler for efficient butt-coupling between compact planar waveguides and single-mode fibers," IEEE J. Quantum Electron. **38**, 949–955, (2002).
10. M. M. Spühler, B. J. Offrein, G.-L. Bona, R. Germann, I. Massarek, and D. Erni, "A Very Short Planar Silica Spot-Size Converter using a Nonperiodic Segmented Waveguide," J. Lightwave Technol. **16**, 1680 (1998).

---

1. Introduction

Like the shrinking of electronic building blocks led to massive integration in electronics, nanophotonics promises similar scaling for photonics. One of the main reasons for the current lack of integration in photonics is that simple waveguides, the core elements on a photonic integrated circuit (PIC), need to make large bends to keep the light confined. This is because the confinement is largely determined by the index contrast between waveguide core and cladding. In semiconductors, this index contrast can be increased by etching deeper into the substrate. To keep such waveguides single-mode, the dimensions must be kept small. For very high contrasts, like semiconductor ($n = 3.45$) to air ($n = 1.0$), waveguides have submicron dimensions, making them hard to define with conventional optical lithography. In addition, the small feature sizes make the coupling to single-mode fibers, with core diameters of $10\mu m$, very difficult.

There are two techniques to design these ultra-compact waveguides. One can use a scaled down version of conventional index-guided waveguides. These *photonic wires* are typically $300 - 500nm$ wide. Alternatively, light can be guided in a photonic crystal, a periodic structure with a high refractive index contrast and a period of the order of the wavelength of the light[1]. This strong contrast and periodicity can create a photonic band gap (PBG), i.e. a wavelength range where light cannot propagate through the crystal. A waveguide can be made by confining the light to a line defect in a photonic crystal. Because of the PBG, bends in photonic crystals can, in principle, be very abrupt.

In a photonic crystal slab, a 2-D periodic structure is used, and in the third, vertical, direction, the light is confined in a simple slab waveguide. These structures can be fabricated using high-resolution lithography and dry etching in a semiconductor layer stack.

At $1.3\mu m$ and $1.55\mu m$, both photonic wires and photonic crystals have dimensions of a few hundred nanometers. However, the accuracy required of the fabrication is of the order of $10nm$. Therefore, we can rightfully speak of nanophotonics. For research purposes, nanophotonic components are traditionally fabricated using e-beam lithography. While this is a very accurate technique, it is slow and unsuitable for mass-fabrication. Conventional photolithography, as used for the fabrication of current photonic ICs, lacks the resolution to define nanophotonic structures. Deep UV lithography at $248nm$ or $193nm$, the technology used for advanced CMOS fabrication, offers both the resolution and throughput needed for commercial applications.

In this paper we will discuss nanophotonic structures for integrated circuits, fabricated with deep UV lithography. We demonstrate photonic wires and photonic crystals in SOI, and interference-based spot-size converters and grating structures for interfacing with optical fibers.

2. Fabrication with deep UV lithography and dry etching

For our high-contrast photonic structures, we use *Silicon-on-Insulator* (SOI). The top Silicon layer provides a good waveguide core, because its high refractive index ($n = 3.45$) contrasts very well with the underlying oxide ($n = 1.45$). To optically separate the guiding top layer from the substrate, the oxide should be sufficiently thick. For our experiments, we ordered commercial wafers from SOITEC fabricated with the UNIBOND® process [2] with a Silicon thickness of $220nm$ and an oxide layer of $1\mu m$.

2.1. Deep UV Lithography

For our experiments we used the advanced CMOS research environment of IMEC, Belgium. We used an ASML PAS5500/750 deep UV stepper at $248nm$. The fabrication process is illustrated in Fig. 1. First, a $200mm$ SOI wafer is coated with photoresist, pre-baked, and given a top AR coating. Then the stepper illuminates the photoresist, which is then baked again, and developed. We used Shipley UV3 resist which is used directly as an etch mask.
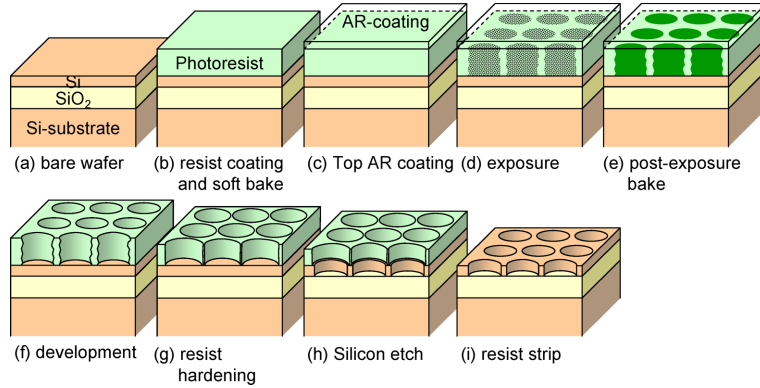
Fig. 1. Fabrication process for photonic nanostructures in SOI using deep UV lithography and dry etching.

Photonic nanostructures typically consist of a variety of structures and for accurate alignment all nanostructures should be printed in the same lithography step. This is not trivial, as not all structures print on target for the same lithography conditions. Especially the exposure dose, i.e. the amount of light in the photoresist, has a large influence on the feature size [3, 4]. For higher doses, the illuminated areas, like the holes of a photonic crystal or the trenches adjacent to photonic wires, will expand. The dose-to-target for photonic crystals and photonic wires can therefore differ significantly. To fabricate both simultaneously, a bias needs to be applied to one or the other, preferably the isolated wires.

As this bias between lines and holes needs to be applied directly on the photomask, it should be known in advance. Therefore, we have included on our first photomask a large number of test structures, representative of many nanophotonic circuit elements. From this, we could extract the necessary bias on the etched features. Fig. 2 shows the required line width (1X on mask) to print a line at a given target width as a function of exposure dose. As an example, the dose-to-target for a triangular lattice of 300nm holes with 500nm pitch is also indicated. At that exposure dose, a bias of 50nm needs to be applied to a 500nm line to print it correctly.

2.2. Etching

After lithography, the patterns in the photoresist are transferred to the underlying SOI by dry etching. We can choose between etching only the top Silicon, or the underlying oxide as well. For a nanophotonic waveguide, etching the oxide is better, as it increases the lateral and the vertical index contrast. For our first experiments [3], we etched the top Silicon layer with a low pressure/high density ICP etch based on $Cl_2/HBr/He/O_2$. This is a highly selective etch process. Subsequently, the oxide was etched using medium density CF_4/O_2-plasma chemistry at medium pressure. In between the etch processes, the wafer is not exposed to the outside atmosphere. However, as we can see in Fig. 3(a), this deep etching causes considerable sidewall roughness[4], because of the limited thickness of the photoresist which is used as an etch mask.

The sidewall roughness can be reduced by thermal oxidation of the top Silicon layer [5]. However, this technique only reduces roughness in the top layer, not in the underlying oxide.

A better solution is not to etch the buried oxide altogether, as shown in Fig. 3(b). In our optimized fabrication process, a plasma treatment of the photoresist is carried out, which smoothens irregularities present in the photoresist patterns. Then the top Silicon is etched
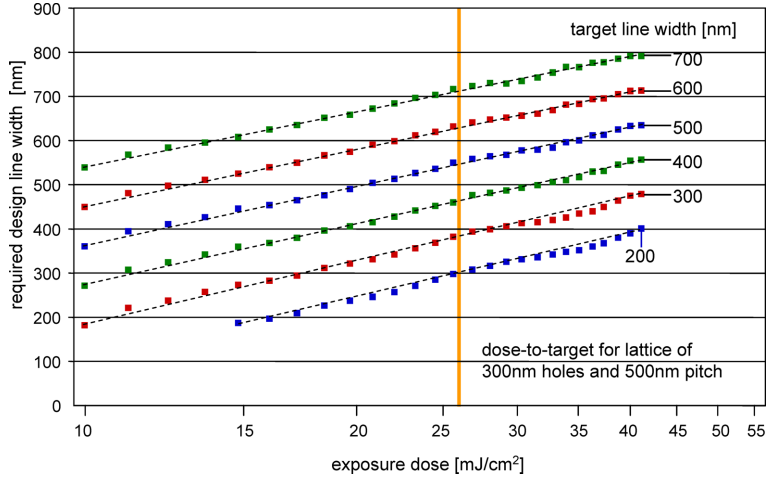
Fig. 2. Linewidth on mask (1X) required to print a line with a given target linewidth at a certain exposure dose. The dose required to print a triangular lattice of 300*nm* holes with a 500*nm* pitch on target is also indicated.
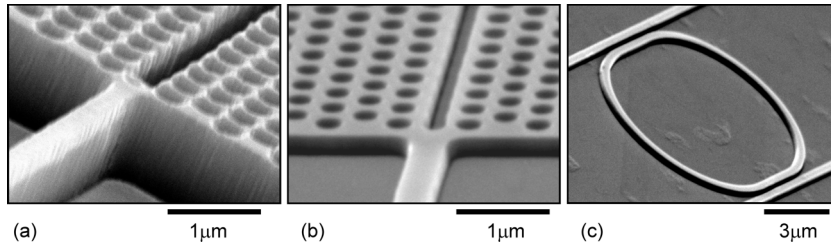
Fig. 3. Photonic crystal waveguides fabricated with deep UV lithography and dry etching. (a) a deeply-etched photonic crystal waveguide with trench defect, (b) the same structure with Silicon-only etch, (c) a racetrack resonator with Silicon-only etch

3. Nanophotonic waveguides

3.1. Measurement setup

To characterize the nanophotonic waveguide components, we measured the transmission of light through the component as a function of wavelength. Light from a tunable laser with a wavelength range from 1500*nm* to 1640*nm* is coupled into a 3μm wide ridge waveguide which is tapered down to a single-mode photonic wire. At the outcoupling side, a taper guides the light back to a 3μm ridge and a high-NA objective collects the light at the outcoupling facet and projects it onto a power detector.

3.2. Photonic wires

Because of their small core and high confinement, photonic wires are an ideal structure to test the fabrication quality. Also, they are ideal to make compact ring and racetrack resonators. We extracted the propagation loss of the wires from the transmission of the Fabry-Perot cavity formed by the incoupling and outcoupling facet. Such spectra (from a 500*nm* wide, Silicon-only etched wires with a length of 10,200,1000μm are plotted in Fig. 4(a). From the fringe contrast P_{max}/P_{min} on the Fabry-Perot spectrum, we can extract the overall losses of the cavity [6], including the transmission at the cleaved facets. When we now plot these losses for cavities
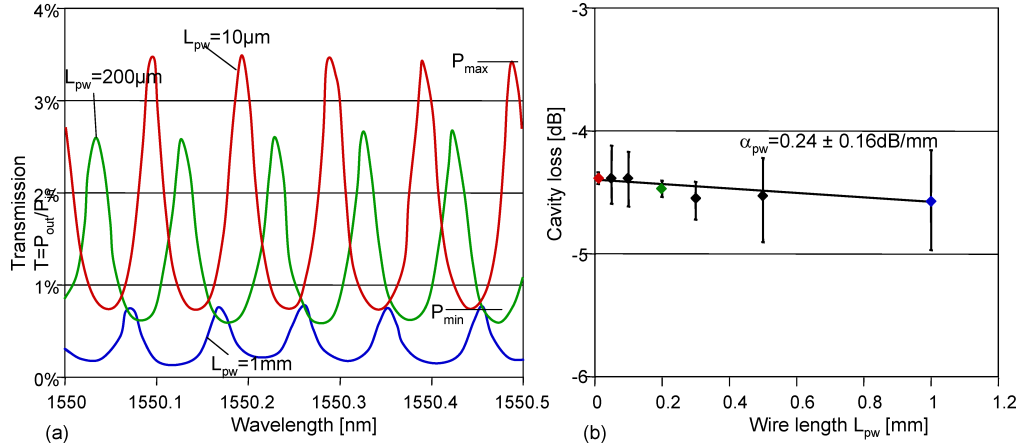
Fig. 4. (a) Transmission spectrum of a Fabry-Perot cavity containing a 500nm wide photonic wire with a wire length L_{pw} of 10μm, 200μm and 1mm. The cavity is 5mm long and the mirrors are formed by the cleaved SOI facets. (b) Cavity loss, expressed in dB, as a function of wire length L_{pw}. The slope of the fitted line gives the propagation loss of the photonic wire in dB/mm.

containing wires of different length, as shown in Fig. 4(b), we can extract the propagation losses of the wires [7]. We used various wire lengths between 10μm and 1mm.

For the deeply etched photonic wires we measured propagation losses of 30dB/mm for 500nm wide (single-mode) wires and 6dB/mm for 600nm wide (bimodal) wires.

When we etch only the Silicon, sidewall roughness improves dramatically. For 500nm wide wires, we now measure 0.24dB/mm, a 25-fold improvement on the deeply etched structures. As the wire gets narrower, losses increase exponentially, with 0.74dB/mm for 450nm wires and 3.4dB/mm for 400nm wires [7, 4]. The wires become multi-mode for widths larger than 550nm.

We have also measured the transmission of ring resonators. For the racetrack resonator illustrated in Fig. 3(c) we found well defined transmission peaks with a quality factor $Q = 3000$ and a drop efficiency of over 80%. This is clear from the measurement spectrum in Fig. 5. The resonator has a bend radius of 5μm and a straight coupling section of 3μm [7].

3.3. Photonic crystal waveguides

Fig. 3(a-b) shows two examples of a photonic crystal waveguides fabricated with deep UV lithography. For the deeply etched structures, the losses are again excessive because of scattering at the rough sidewalls. For a simple W1 waveguide with a lattice period of 500nm and a hole size of 320nm we measured waveguide losses of 21dB/mm in a PBG-guided mode [4].

For the structures with a Silicon-only etch, the sidewall roughness is strongly reduced, with a positive effect on the propagation losses. For a W1 waveguide (a waveguide consisting of a line defect in the photonic crystal where a single row of holes is removed), we measured significant transmission through a 1mm long waveguide. Fig. 6 shows a W1 photonic crystal waveguide with a lattice pitch $a = 500nm$ and a hole diameter of 320nm and its propagation losses. These results are obtained by measuring the transmission through waveguides of various length, after filtering out the oscillations due to the multiple cavities formed by the facets and the interfaces between the photonic wires and the photonic crystal waveguides. Around 1525nm, the odd mode is guided and has a propagation loss as low as 7.5dB/mm, which is much lower than the
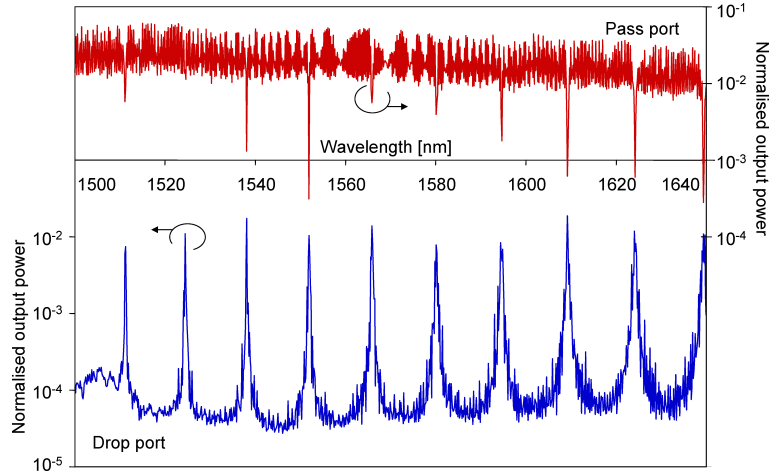
Fig. 5. Transmission spectrum of the racetrack resonator from Fig. 3(c) in the pass port and the drop port. The resonator has a Q of over 3000 and a coupling efficiency at resonance of 80%.
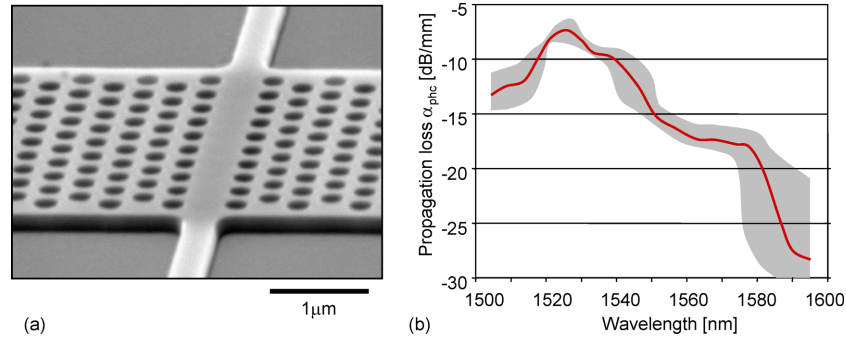
Fig. 6. Propagation losses of a W1 photonic crystal waveguide with Silicon-only etch. The lattice has a pitch of 500nm and the holes a diameter of 320nm.

propagation losses of the deeply etched structures. Also, the other cavity losses have dropped with a few dB.

4. Interfacing to optical fibers

Because of the small (submicron) core dimensions of a nanophotonic waveguide, the coupling from and to optical fibers is not straightforward. Adiabatic tapers can widen the waveguide mode, and coupling structures with multi-layer taper structures to expand the mode vertically have been demonstrated [8], but these structures require a long transition length and therefore a large footprint on the chip, something which is undesirable for integrated nanophotonics.

4.1. Grating-based fiber coupler

Because Silicon-on-insulator has only a thin core layer, butt-coupling to a single-mode fiber introduces unacceptable losses, even from a $10\mu m$ wide ridge waveguide. We have demonstrated a fiber coupler consisting of a second-order diffractive grating to couple from a broad ridge waveguide to a vertically oriented, butt-coupled single-mode fiber [9]. The principle is
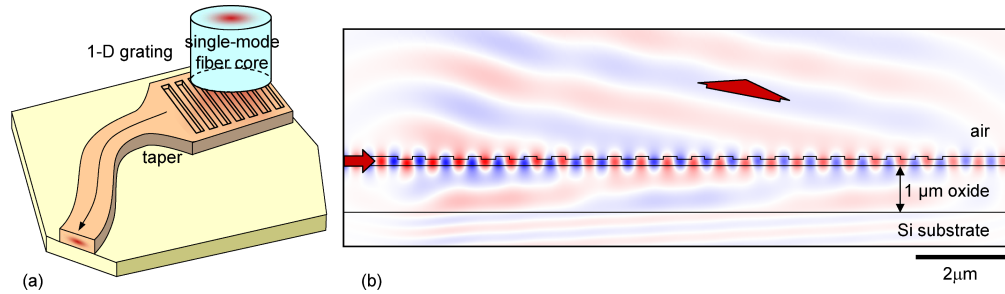
Fig. 7. Fiber coupling structures in Silicon-on-insulator. (a) concept, (b. 239KB) Simulation of a 1-D grating, coupling from a waveguide to a fiber under a 10° angle.
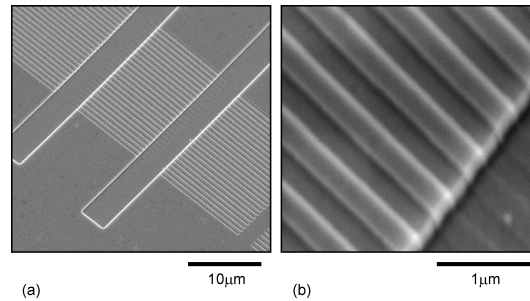
Fig. 8. SEM micrographs of a fiber coupling grating in Silicon-on-insulator. The grating etch is not as deep as the waveguide trenches.

illustrated in Fig. 7(a). Although the grating is etched only $50nm$ into the Silicon, it is a strong grating, as the etch depth is a significant fraction of the $220nm$ core thickness. Theoretical calculations show that this grating can couple more than 30% of the light to and from the fiber. Fig. 7(b) shows an animated field plot of light coupled from an SOI waveguide to a fiber which is tilted 10° off the vertical. When enhanced with an optimized multi-layer SOI stack and an additional first-order grating, the efficiency can be boosted to more than 70%.

Because these fiber couplers require a different etch depth than the other, high-contrast structures, they are to be fabricated in a separate process step. Fig. 8 shows such a fiber coupler with an etch depth of $50nm$ in a broad ridge waveguide with an etch depth of $220nm$. For the alignment, we use the built-in capabilities ($< 50nm$) of the deep UV stepper.

To measure the coupling efficiency, we used these fiber couplers to couple light into a $10\mu m$ wide ridge waveguide, which is then tapered to a single-mode wire ($500nm$) to filter out the (small) coupling to higher-order waveguide modes, as shown in Fig. 9(a). Then, the waveguide is again expanded and an identical grating is used for outcoupling. Fig. 9(b) shows the coupling efficiency of a single coupler extracted from such a transmission measurement. The $-6.8dB$ peak transmission corresponds to a coupling efficiency of 21% per coupler. The $3dB$ bandwidth of a single coupler is $60nm$. Similar, e-beam-fabricated structures have shown coupling efficiencies of 25%.

4.2. Compact spot-size converters

To couple light from a single-mode photonic wire to a $10\mu m$ wide waveguide, an adiabatic taper should be several hundred μm long. A non-adiabatic taper based on multi-mode interference can couple a broad and narrow waveguide over a much shorter length [10]. An example with
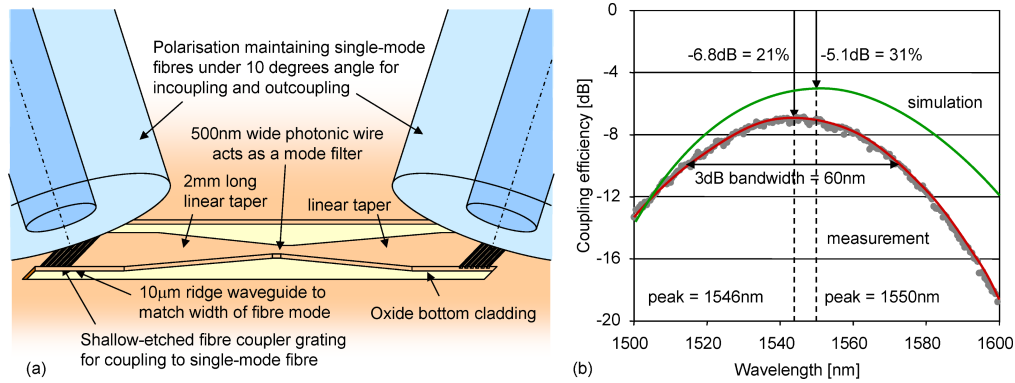
Fig. 9. Measurement of fiber coupling gratings. (a) measurement scheme, (b) coupling efficiency of a single fiber couples extracted from the fiber-to-fiber transmission measurement, compared to the simulation results.
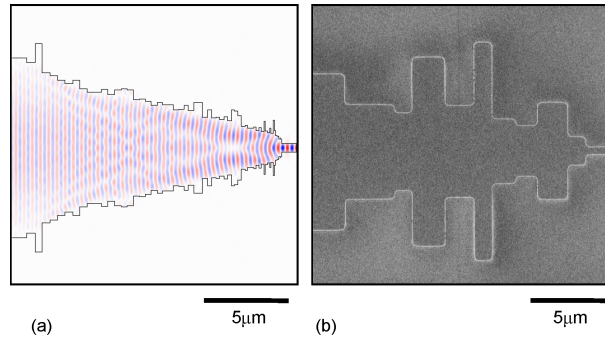
Fig. 10. Short spot-size converter between a $10\mu m$ wide ridge waveguide and a $500nm$ wide photonic wire. (a. 539KB) Simulation result, (b) a fabricated structure

an animated field plot is shown in Fig. 10(a). The coupler consists of a non-periodic segmented waveguide. Because each segment is actual a multi-mode waveguide, the various waveguide modes will interfere. In this sense, the structure is a generalized multi-mode interferometer (MMI). After optimization of the segments' width and length using both genetic algorithms and a steepest-descent method, the interference pattern of at the end of the structure is matched to the mode in the photonic wire. As this optimization is purely neumerical, it is not straightforward to gain insight into the design of these structures. With this technique we have calculated transmissions over 90%.

Fig. 10(b) shows an SEM picture of a spot-size converter of $15\mu m$ long in SOI with only 10 sections. We plotted the transmission of a waveguide with this structure in Fig. 11(b). Light is coupled with a vertical fiber coupler into a $10\mu m$ wide waveguide, which in turn, is coupled to a $550nm$ waveguide with a spot-size converter, and with the same scheme in reverse for outcoupling, as shown in Fig. 11(a).

As a comparison, we also plotted the transmission of a similar structure, but with a $50\mu m$ long linear taper. The reference transmission curve (fiber-to-fiber) of the fiber couplers is also plotted. At its maximum, the transmission curve of the interference coupler is 3dB below the reference curve, which for a single interference taper translates into a coupling efficiency of more than 70%. we also see that this spot-size converter performs roughly equal to the 3 times longer linear taper. This coupling efficiency is roughly constant over a wavelength range of
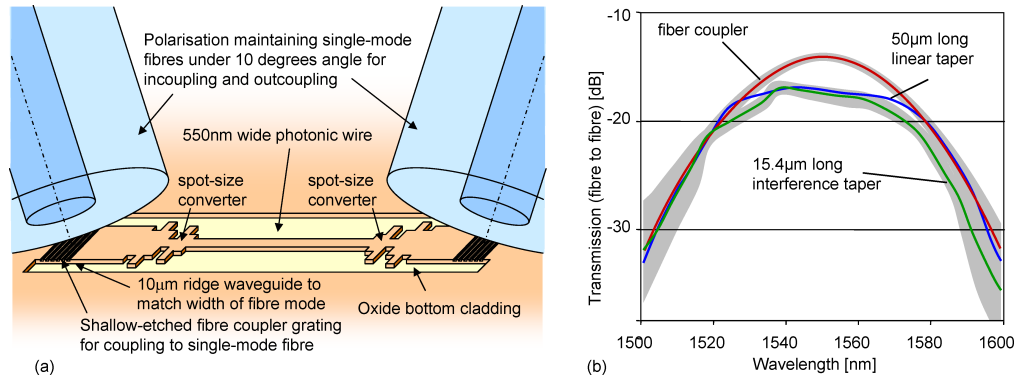
Fig. 11. Measurement of spot-size converters between a $10\mu m$ wide ridge waveguide and a $500nm$ wide photonic wire. (a.) Measurement scheme (b) fiber-to-fiber transmission measurement (using fiber couplers) of the structure from Fig. 10(b), compared to a $50\mu m$ linear taper.

$50nm$ $(1525nm - 1575nm)$.

5. Conclusion

We have demonstrated the use of deep UV lithography for the fabrication of nanophotonic waveguide structures and characterized a number of components. For photonic wires, propagation losses are as low as $0.24dB/mm$ for a wire width of $500nm$, while for photonic crystals, losses as low as $7.5dB/mm$ have been demonstrated.

We have also designed and fabricated mode converters and grating structures to facilitate the interface to single-mode fiber. Our experimental results show a coupling efficiency of over 21% to and from a single mode fiber to a $10\mu m$ wide SOI ridge waveguide. Interference-based spot-size converters with a coupling efficiency of 70% have also been demonstrated.